Journal of the Association of Arab Universities for Basic and Applied Sciences (2015) **18**, 19–28

University of Bahrain

Journal of the Association of Arab Universities for Basic and Applied Sciences

www.elsevier.com/locate/jaaubas
www.sciencedirect.com

صياغات تحليلية للتعبير عن كيفية التخلص من تراكيز أوكسيد النيتريك في الطور الغازي وفي طور الغشاء الحيوي في المرشحات البيولوجية ذات الجريان المتقطع

Rasi Muthuramalingam [b], Sunil Kumar [a], Rajendran Lakshmana [b,*]

[a] Department of Mathematics, National Institute of Technology, Jamshedpur 831014, Jharkhand, India
[b] Department of Mathematics, The Madura College, Madurai 625011, Tamil Nadu, India

الملخص:

تطرح هذه الورقة استعمال أنموذج رياضي لإزالة أوكسيد النيتريك باستعمال مرشح حيوي ذي الجريان المتقطع معبأ بدقائق منتظمة من السيراميك تحت ظروف أليفة للحرارة. والأنموذج المقترح هنا مبني على انتقال الكتلة ما بين واجهة الغاز والغشاء الحيوي والأكسدة الكيميائية في الطور الغازي. تم اشتقاق هذه الصياغات التحليلية لتراكيز أوكسيد النتريك في الطوري الغازي وطور الغشاء الحيوي باستعمال طريقة أدوميان للإنحلال لكل قيم المتغيرات الممكنة. بالإضافة إلى ذلك فقد تمت المحاكاة الرقمية للمسألة المطروحة باستعمال برنامج ماتلاب بغرض تقصى دينامية النظام المتبع. كما أن النتائج التخطيطية قد تم طرحها ومناقشتها كمياً لتوضيح الحل المطروح. وقد تم الحصول على توافق بين الحلول والنتائج النظرية في هذه الدراسة.

Journal of the Association of Arab Universities for Basic and Applied Sciences (2015) **18**, 19–28

University of Bahrain

Journal of the Association of Arab Universities for Basic and Applied Sciences

www.elsevier.com/locate/jaaubas
www.sciencedirect.com

ORIGINAL ARTICLE

Analytical expressions for the concentration of nitric oxide removal in the gas and biofilm phase in a biotrickling filter

Rasi Muthuramalingam [b], Sunil Kumar [a], Rajendran Lakshmanan [b,*]

[a] *Department of Mathematics, National Institute of Technology, Jamshedpur 831014, Jharkhand, India*
[b] *Department of Mathematics, The Madura College, Madurai 625011, Tamil Nadu, India*

Received 31 August 2013; revised 8 March 2014; accepted 27 March 2014
Available online 24 April 2014

KEYWORDS

Nitric oxide;
Biotrickling filter;
Mathematical modelling;
Adomian decomposition method

Abstract In this paper, a mathematical model of nitric oxide removal using biotrickling filter (BTF) packed with uniform ceramic particles under thermophilic condition is discussed. The model proposed here is based on the mass transfer in gas-biofilm interface and chemical oxidation in the gas phase. Analytical expressions pertaining to the nitric oxide (NO) concentration in the gas and bio-film phase have been derived using the Adomian decomposition method (ADM) for all possible values of parameters. Furthermore, in this work the numerical simulation of the problem is also reported using Matlab program to investigate the dynamics of the system. Graphical results are presented and discussed quantitatively to illustrate the solution. Good agreement between the solutions is presented in this paper and numerical data are obtained.

1. Introduction

Rapid increases in the emission of nitrogen oxides (NO_x) can adversely affect human health, damage crops, and are implicated in the formation of acid rain (Van Langenhove et al., 1986). Nitrous oxide, a chemical compound with the formula N_2O is one of the NO_x components which are known as laughing gas in common. It is an oxide of nitrogen. At room temperature, it is a colourless, non-flammable gas, with a slightly sweet odour and taste. Nitrous oxide is a long-lived greenhouse gas, with a direct global warming potential 298 times higher than that of carbon dioxide (Solomon et al., 2007). Therefore, even low amounts of N_2O emission are unwanted. Nitrous oxide gives rise to nitric oxide (NO) on reaction with oxygen atoms and this NO in turn reacts with ozone. Nitric oxide which is the major component of nitrogen oxide reacts with moisture in the air to form nitrous acid which is a major constituent of acid rain.

In order to control the emission of volatile organic compounds (VOC) like nitrous oxide, nitric oxide, toluene etc. from industries, biofilters are being used nowadays instead of the chemical complex absorption method (Islam and Alam, 2006; Vafajoo et al., 2012). Biofilters offer two major

* Corresponding author. Tel.: +91 9442228951; fax: +91 0452 2675238.
E-mail addresses: rasildc@gmail.com (R. Muthuramalingam), skumar.math@nitjsr.ac.in, skiitbhu28@gmail.com (S. Kumar), raj_sms@rediffmail.com (R. Lakshmanan).
Peer review under responsibility of University of Bahrain.

1815-3852 © 2014 Production and hosting by Elsevier B.V. on behalf of University of Bahrain.
http://dx.doi.org/10.1016/j.jaubas.2014.03.003

advantages to an energy-starved country like India. Their power consumption is very low (1.8–2.5 Kwh/1000 m^3) compared with other technologies. Secondly, their capital operating costs are very low which can be an added boon to our industry, which opt for high economic pollution control technologies (James and Natalve, 1996). Biofiltration is a complex process with many physical, chemical, and biological phenomena (Devinny et al., 2002). In biofiltration the contaminated air is passed through a packed bed where biodegradable gases or volatile compounds are absorbed into the biofilm (Baquerizo et al., 2005).

Biofiltration has become one of the leading technologies for controlling VOC emissions (Zarook and Shaikh, 1997; Cox and Deshusses, 1998). There are three conventional types of biofilter: biofilter, trickling biofilter and bioscrubber. Biotrickling filters have been shown in several instances to be superior to biofilters when accurate control of the environmental conditions or higher pollutant elimination rates are required (Baltzis et al., 2001). Moreover, biotrickling filters packed with better structural strength can be built taller than biofilters (Cox et al., 2001). A liquid stream trickles through the porous packed bed and provides nutrients without carbon to the micro-organisms. The micro-organism in the biofilm degrades the biodegradable pollutants in waste gas while it passes through the packed bed and diffuses through the attached biofilm. Biotrickling filters are relatively new and are still regarded as an emerging technology for air pollution control (Liao et al., 2008). Biotrickling filters require low maintenance (Deshusses Marc et al., 2004). Biotrickling filters are increasingly used in industrial applications.

NO removal by applying some thermophilic microorganisms in various temperatures was studied experimentally by Flanagan and Lee (Flanagan et al., 2002; Lee et al., 2001). Besides, theoretical modelling studies regarding NO removal in BTF reactor are very limited due to the non linear character of mass balance equations over the biofilm phase. Caceres, Song and Zarook analysed the BTF modelling on removal of volatile organic compounds (Caceres et al., 2012; Song and Kinney, 2002; Zarook and Shaikh, 1997). Liang et al. (2012) developed a mathematical model for nitric oxide removal in a biotrickling filter under thermophilic conditions. Matlab software package was employed to acquire the numerical solution of the model. However to the best of our knowledge, no rigorous analytical expressions of concentration of nitric oxide in the gas phase and in the biofilm phase have been reported (Liang et al., 2012). The purpose of this communication is to derive the approximate analytical expressions for the nitric oxide concentration in both the phases using the Adomian decomposition method.

2. Mathematical modelling

The experimental setup for the BTF reactor is given in Fig. 1. The BTF was constructed with cylindrical plexiglass. The height and diameter of the reactor were 50 and 8 cm, respectively. The packing space was at the height from 10 to 40 cm calculated from the bottom of the BTF. The outer layer of the reactor was shielded with a heat tape which is covered with a layer of fibreglass insulator. The reactor temperature was maintained at 50 ± 1 °C. The experiment was conducted in two experimental phases. In the first phase, the characteristics of *Chelatococcus daeguensis* in anaerobic environment in the presence of nitrate were found out. In the second phase, the potentiality of immobilization material in the biofilter which could adsorb NO_2 gas effectively as well as possess good bacterial immobilization capacity was identified (Islam and Alam, 2006). Let us consider the mass balance equations for

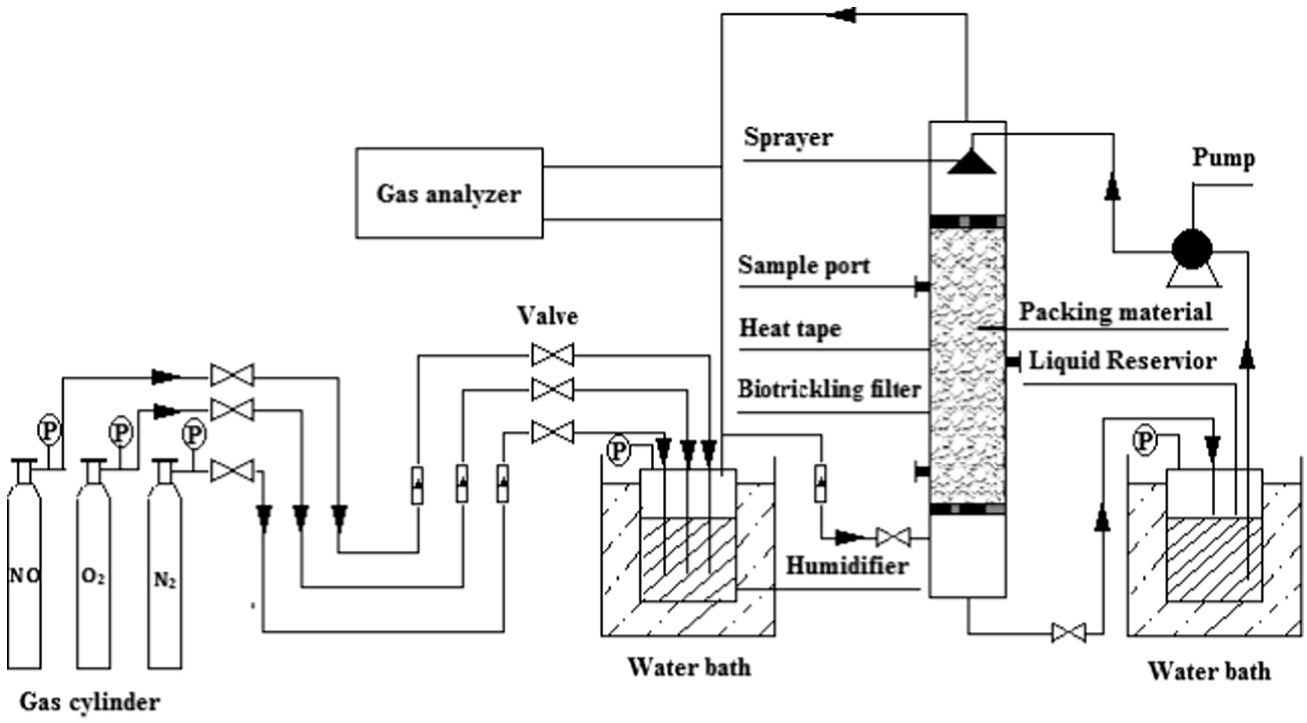

Figure 1 Experimental setup of a biotrickling filter system (Liang et al., 2012).

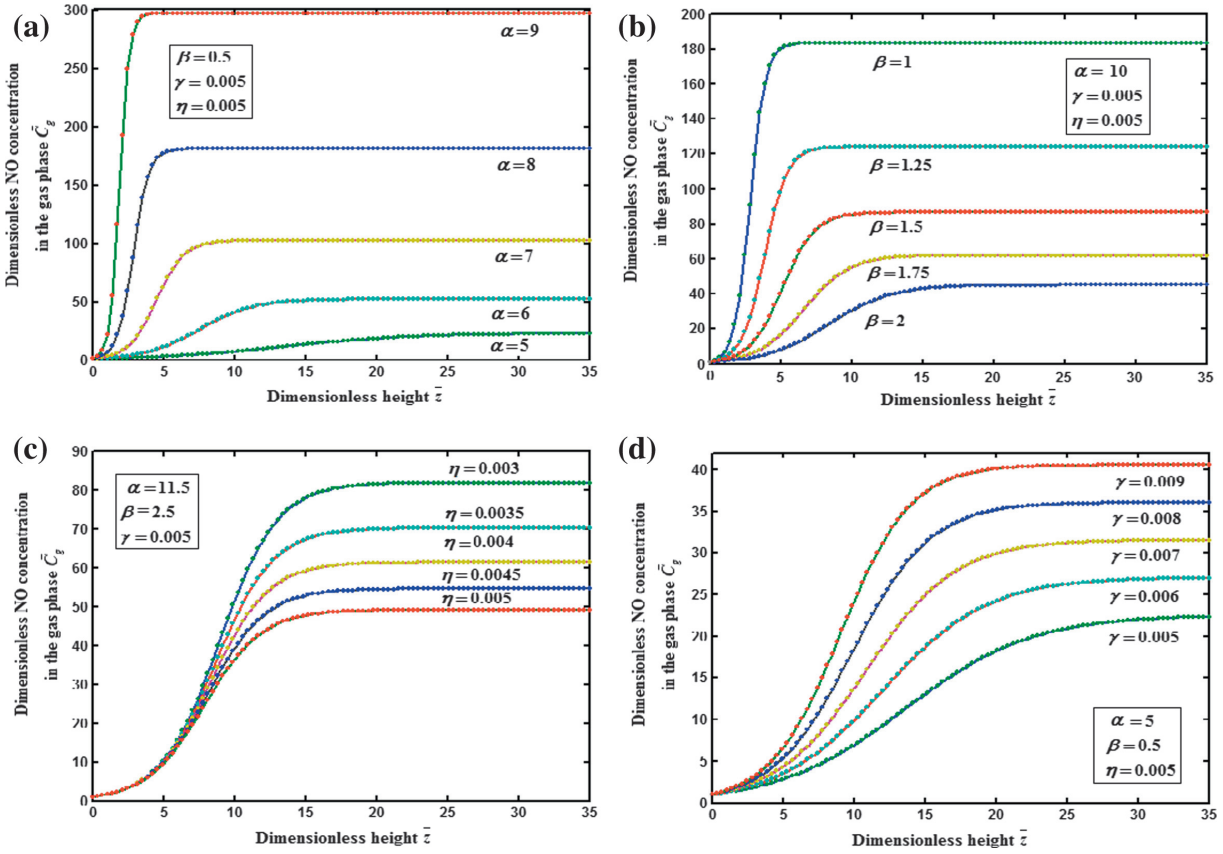

Figure 2 Dimensionless NO concentration in the gas phase ($\bar{C}_g$) versus dimensionless height z for various values of α, β, η and γ and for some fixed values of other parameters. The key to the graph: solid line represents the Eq. (12) and dotted line represents the numerical simulation.

micro-volume units in the gas phase and the biofilm phase respectively on the basis of operation conditions in Liang et al. (2012) as follows:

Mass balance equation over the gas phase:

$$U_g \frac{dC_g}{dz} = a_f \, D_e \frac{dC_l}{dx}\bigg|_{x=0} - 2k_g C_g^2 \varepsilon_f \tag{1}$$

where U_g is the superficial gas velocity; C_g is the NO concentration in the gas phase and C_l is the NO concentration in the biofilm phase; a_f is the specific surface area of biofilm; D_e is the effective diffusion coefficient in the biofilm; k_g is the reaction rate constant; ε_f is porosity ratio of biofilm covered packing materials; $-D_e \frac{dC_l}{dx}\big|_{x=0}$ is the flux across the gas biofilm interface; z is the height value which is calculated from the base of the packing materials; x is the coordinate axis which is calculated from the surface of the biofilm. The equation (Eq. (1)) must be solved to the boundary condition

$$C_g = C_{g,0} \quad \text{at } z = 0, \tag{2}$$

Mass balance equation over the biofilm phase is

$$D_e \frac{d^2 C_l}{dx^2} = \frac{\mu_m}{Y} \frac{C_l}{K_s + C_l} X_V \tag{3}$$

where X_V is the microbial density of the biofilm; K_s is the Monod half saturation constant; μ_m is the maximum specific growth rate of biomass; Y is the yield coefficient of micro-organisms; μ_m/Y gives the maximum specific substrate utilization rate. Boundary conditions for Eq. (3), are given by

$$C_l = C_g/H \quad \text{at } x = 0 \tag{4}$$

$$\frac{dC_l}{dx} = 0 \quad \text{at } x = L_f \tag{5}$$

where H is Henry constant at 50 °C and L_f is the biofilm thickness. The NO concentrations in both the gas and biofilm phase were analysed experimentally by a flue gas analyser (TESTO 350Pro, Germany) at 10 h intervals (Liang et al., 2012).

2.1. Dimensionless form

The non-linear differential Eqs. (1) and (3) are made dimensionless by defining the following parameters:

$$\begin{aligned} &\bar{C}_l = \tfrac{C_l}{C_g/H}, \quad \bar{x} = \tfrac{x}{L_f}, \quad \alpha = L_f\sqrt{\tfrac{\mu_m}{Y}\tfrac{X_V}{D_e K_s}}, \quad \beta = \tfrac{C_g/H}{K_s}, \\ &\bar{C}_g = \tfrac{C_g}{C_{g,0}}, \quad \bar{z} = \tfrac{z}{L_f}, \quad \gamma = \tfrac{a_f D_e}{HU_g}, \qquad\qquad \eta = \tfrac{\varepsilon_f k_g C_{g,0} L_f}{U_g} \end{aligned} \tag{6}$$

Using the above dimensionless variables, Eqs. (1) and (3) reduce to the following dimensionless form:

$$\frac{d\bar{C}_g}{d\bar{z}} = \gamma \bar{C}_g \frac{d\bar{C}_l}{d\bar{x}}\bigg|_{\bar{x}=0} - 2\eta \bar{C}_g^2 \tag{7}$$

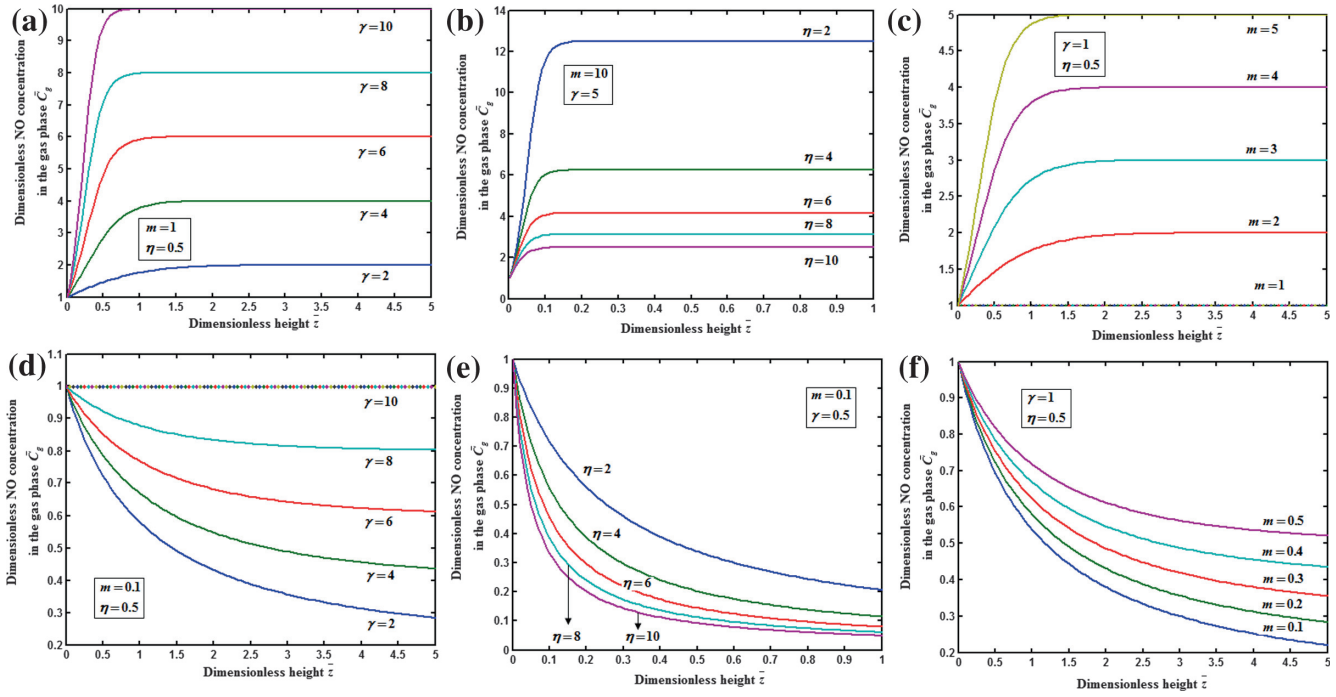

Figure 3 Dimensionless NO concentration in the gas phase ($\bar{C}_g$) versus dimensionless height ($\bar{z}$) for various values of γ, η and (m) and for some fixed values of other parameters. The key to the graph: solid line represents the Eq. (12) and dotted line represents the numerical simulation.

$$\frac{d^2\bar{C}_l}{d\bar{x}^2} = \frac{\alpha^2\bar{C}_l}{1+\beta\bar{C}_l} \tag{8}$$

The corresponding boundary conditions for the above Eqs. (7) and (8) can be expressed as

$$\bar{C}_g = 1 \quad \text{at } \bar{z} = 0, \tag{9}$$

$$\bar{C}_l = 1 \quad \text{at } \bar{x} = 0 \tag{10}$$

$$\frac{d\bar{C}_l}{dx} = 0 \quad \text{at } \bar{x} = 1 \tag{11}$$

3. Analytical expressions of concentration of NO in gas and biofilm phase using Adomian decomposition method

In the recent years, much attention is devoted to the application of the Adomian decomposition method to the solution of various scientific models (Adomian, 1984; Mohamed, 2010; Omar Jaradat, 2008; Patel et al., 2011; Siddiqui et al., 2010). The ADM yields an analytical solution in terms of a rapidly convergent infinite power series with easily computable terms and without linearization, perturbation, transformation or discrimination. In this paper, the Adomian decomposition method (see Appendix A) is used to solve non-linear differential equation (Muthukaruppan et al., 2012). The analytical expressions for the concentration of NO in the gas phase $\bar{C}_g$, and in the biofilm phase $\bar{C}_l$, (see Appendix B) are obtained as follows:

$$\bar{C}_g(\bar{z}) = \gamma m e^{\gamma m \bar{z}}\left[\gamma m - 2\eta + 2\eta e^{\gamma m \bar{z}}\right]^{-1} \tag{12}$$

$$\bar{C}_l(\bar{x}) = 1 + \frac{\alpha^2\bar{x}(\bar{x}-2)}{2(1+\beta)} + \frac{\alpha^4\bar{x}[\bar{x}^2(\bar{x}-4)+8)]}{24(1+\beta)^3} \tag{13}$$

where

$$m = \frac{\alpha^4}{3(1+\beta)^3} - \frac{\alpha^2}{(1+\beta)} \tag{14}$$

4. Removal ratio of NO

The percentage of the NO removal ratio (NO removal efficiency NO_R) is (Takao Namihira et al., 2000)

$$NO_R = \frac{NO_i - NO_f}{NO_i} \times 100 \tag{15}$$

where NO_i and NO_f are the initial (before treatment) and the final (after treatment) concentrations of NO in the gas phase, respectively. In the present work, $NO_i = 1$ and $NO_f = \bar{C}_g$.

5. Numerical simulation

In order to investigate the accuracy of the ADM solution with a finite number of terms, the system of differential equations was solved numerically. To show the efficiency of the present method, our results are compared with numerical results graphically. The function pdepe (Finite element method) which is a function of solving initial-boundary value problems for parabolic–elliptic PDEs in 1-D is used to solve Eq. (7) numerically. And Eq. (8) is solved numerically using the Matlab function ode45 (Range–Kutta method) which is a function of solving the initial-boundary value problems in Matlab software (MATLAB 2000, Skeel and Berzins, 1990).

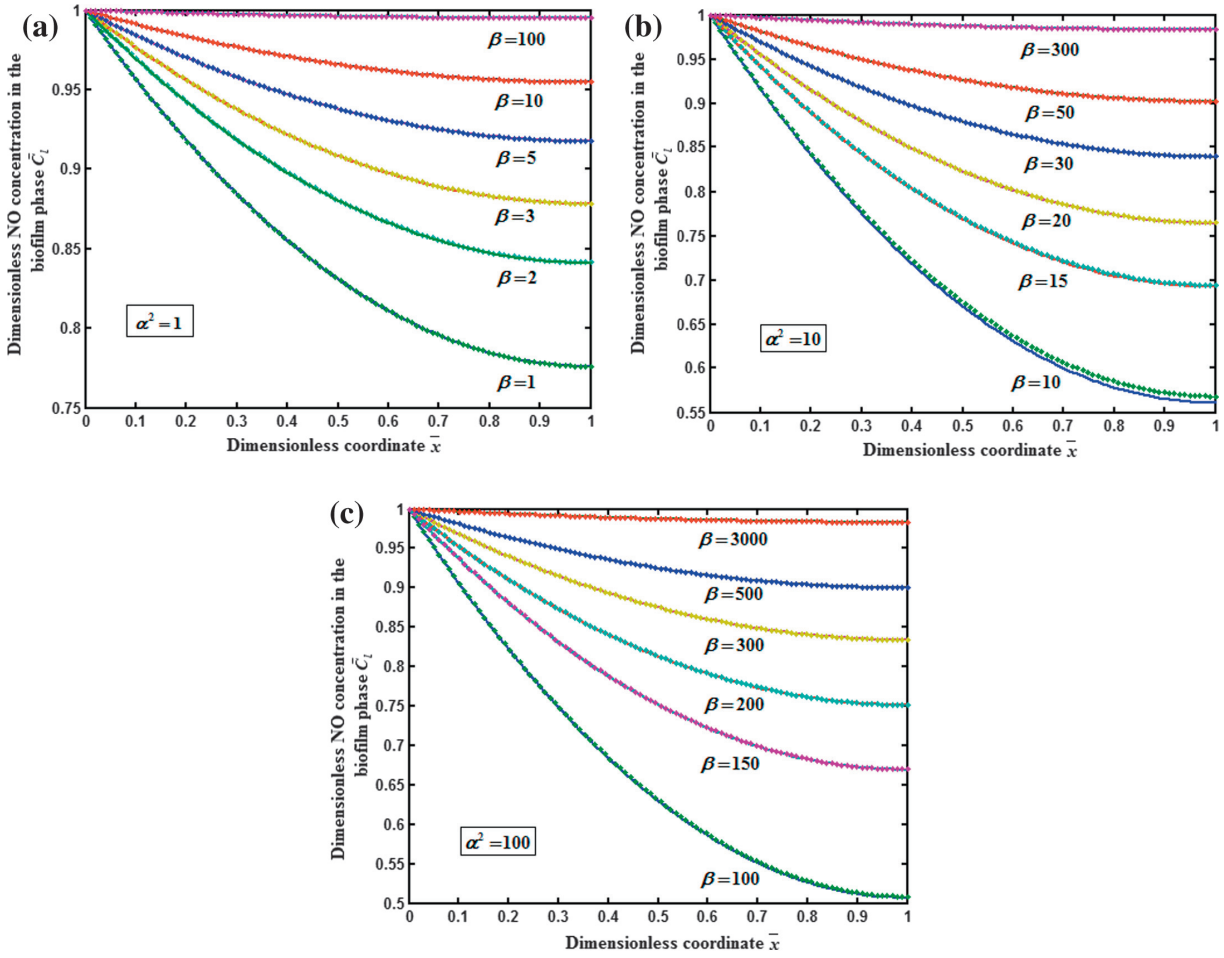

Figure 4 Dimensionless NO concentration in the biofilm phase ($\bar{C}_l$) versus dimensionless coordinate $\bar{x}$ for various values of β and for some fixed values of the parameter α^2. The key to the graph: solid line represents the Eq. (13) and dotted line represents the numerical simulation.

The analytical solutions of NO concentration in the gas phase and the biofilm phase are compared with simulation results in Figs. 1–6 A satisfactory agreement is noted.

6. Results and discussion

Eqs. (12) and (13) represent the simple analytical expressions pertaining to the NO concentration in the gas phase and the biofilm phase respectively. The main variables of interest in this study are the concentration of NO in the gas phase $\bar{C}_g$ and the biofilm phase $\bar{C}_l$ respectively. The concentration of nitric oxide in the gas phase depends on the following four factors γ, η, α and β. The parameter γ depends upon specific surface area of the biofilm a_f, effective diffusion coefficient D_e, Henry constant H and superficial gas velocity U_g. The parameter α and η depends upon the biofilm thickness L_f. And the factor β depend on the inlet NO concentration.

Fig. 2(a) shows the dimensionless concentration profile of NO in the gas phase versus dimensionless height $\bar{z}$ for various values of α. The variation in the dimensionless variable α can be achieved by varying either the thickness or the microbial density of the biofilm. As α increases, the concentration of NO increases for $\bar{z} \leqslant 5$. It indicated that the concentration of NO depends upon the thickness of the biofilm. In Fig. 2(b), the influence of β over NO concentration in the gas phase versus height $\bar{z}$ was analysed. For some fixed values of the parameters the concentration increases when β decreases. From this figure, it is also evident that the concentration is inversely proportional to β. From Fig. 2(c) it is observed that the concentration of NO increased rapidly since $\bar{z} < 15$ and reaches the maximum at $\bar{z} = 15$ and then remains approximately constant. Sharp increases are due to the inlet nitrogen concentration $C_{g,0}$. When η increases the concentration decreases. From this figure, it is deducted that, for minimum values of η the concentration of NO increases. Fig. 2(d) represents the concentration of NO for various values of γ. The variation in γ can be accomplished by changing either the diffusion coefficient in the biofilm, or the superficial gas velocity. From this figure, it is confirmed that the concentration increases when γ (specific surface area of the biofilm) increases with respect to the height $\bar{z}$. In Fig. 3, the concentration of NO in the gas phase $\bar{C}_g$ versus height $\bar{z}$ for various values of parameters γ, η and m is plotted. The concentration of $\bar{C}_g$ increases with the increase of γ, η and m. It reaches the steady state value when $\bar{z} \geqslant 1$ for all values of γ, η and m. For $m < 1$, the concentration decreases for various values of γ and η. And for $m \geqslant 1$, the concentration decreases.

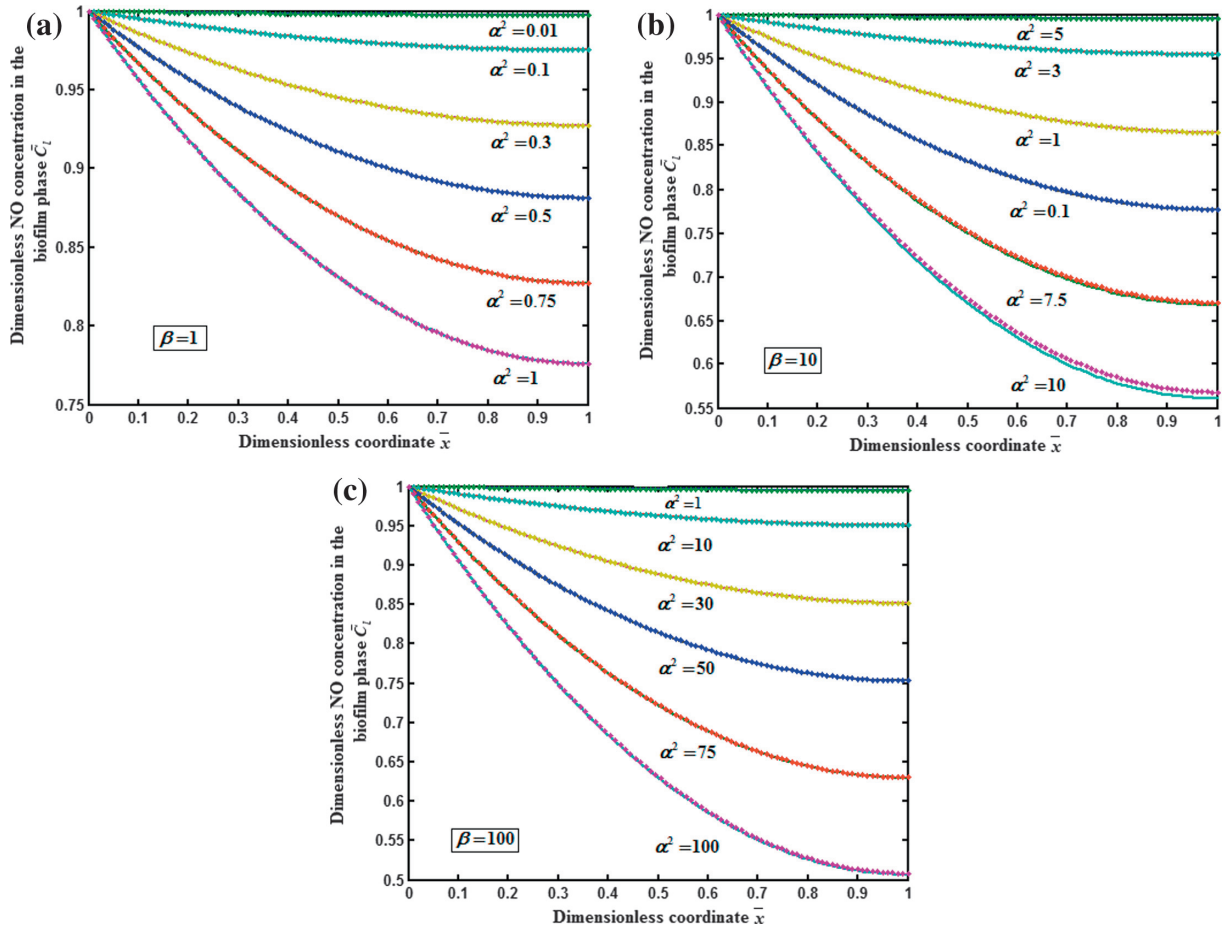

Figure 5 Dimensionless NO concentration in the biofilm phase ($\bar{C}_l$) versus dimensionless coordinate $\bar{x}$ for various values of α^2 and for some fixed values of the parameter β. The key to the graph: solid line represents the Eq. (13) and dotted line represents the numerical simulation.

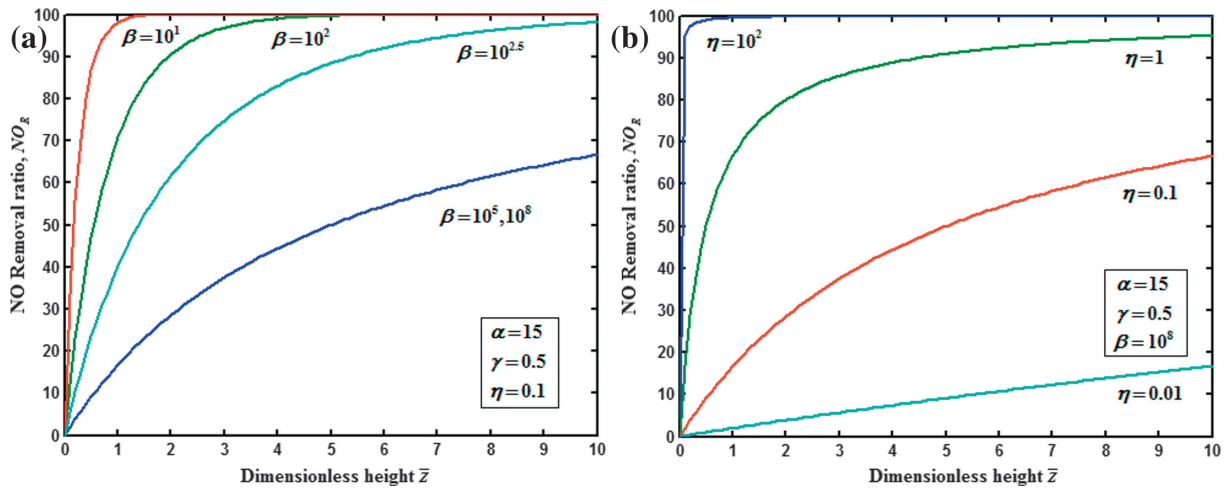

Figure 6 NO Removal ratio NO_R versus dimensionless height $\bar{z}$ for various values of β and η for some fixed values of the other parameters. The graph is plotted using Eq. (15).

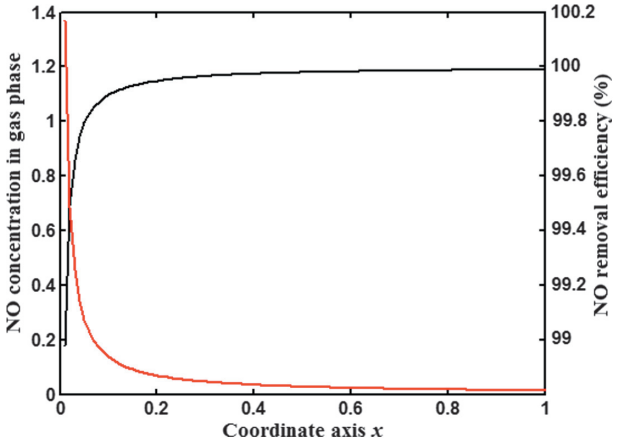

Figure 7 NO concentration and Removal ratio NO_R versus coordinate axis x for some fixed values of the parameters (refer Table. 1). The graph is plotted using Eqs. (6), (12), and (15).

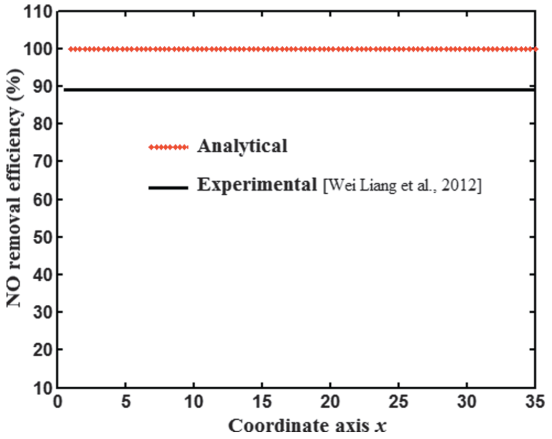

Figure 8 Comparison of experimental and analytical (simulation) results of NO Removal ratio (NO removal efficiency, NO_R) versus dimensionless height x for some fixed values of the parameters (Refer Table. 1). The graph is plotted using Eqs. (6) and (15).

Fig. 4 and 5 exhibit the concentration of NO in the biofilm phase C_l for different values of α^2 and β. From Fig. 4(a)–(c), it is inferred that the concentration of NO increases when β increases for some fixed values of α^2. For large values of β, the concentration remains constant. In Fig. 5(a)–(c), the concentration of NO in the biofilm phase for various values of α^2 and for some fixed values of β is presented. From this figure, we conclude that the concentration of NO increases when thickness of the film decreases.

Fig. 6 illustrates the removal ratio of NO (NO removal efficiency) in the gas phase. From Fig. 6(a) and (b), it is evident that the removal ratio increases when β (half saturation constant increases) decreases and η (biofilm thickness) increases. This shows that NO removal efficiency is inversely proportional to the inlet nitrogen concentration and directly proportional to the biofilm thickness. Fig. 7 depicts that the difference between the experimental and analytical profiles of NO removal efficiency versus the coordinate axis x. Our obtained analytical results are verified.

Fig. 8 shows the profile of NO concentration and NO removal efficiency versus coordinate axis x for experimental values in Table. 1 using Eqs. (6) and (12). It can be seen from Fig. 8 that the concentration of NO decreases with increasing x and accordingly the removal efficiency of NO increases with increasing x. When x is less than 0.4, the decreasing rate of NO concentration or the increasing rate of removal efficiency is comparatively fast; while when x is greater than 0.4, the concentration and removal efficiency of NO reach a steady level.

Table 1 Parameter values used for solving the model equations.

Symbols		Parameters	Formula	Values	Units	Reference
a_0		Specific surface area of medium	Measured experimentally	398	m^{-1}	Liang et al. (2012)
ε_0		Porosity of medium	Measured experimentally	0.62	Dimensionless	Liang et al. (2012)
L		Characteristic length of the vertical channels	$L = 2\frac{\varepsilon_0}{a_0}$	0.003	m	Liang et al. (2012)
a_f		Specific surface area of biofilm	$a_f = a_0\left(1 - \frac{L_f}{L}\right)$	12876.34	cm^{-1}	Liang et al. (2012)
D_e		Effective diffusion coefficient in the biofilm	Measured experimentally	$5.21 * 10^{-5}$	$cm^2\ s^{-1}$	Stewart, (2003), Liang et al. (2012)
k_g		Reaction rate constant	Arrhenius equation	$6.496 * 10^3$	$L^2\ mol^{-2}\ s^{-1}$	Liang et al. (2012), Nagase et al. (1997)
ε_f		Porosity ratio of biofilm covered packing materials	$\varepsilon_f = \varepsilon_0\left(1 - \frac{L_f}{L}\right)^2$	648	Dimensionless	Liang et al. (2012)
L_f		Biofilm thickness	Measured experimentally	0.1	cm	Liang et al. (2012), Chen et al. (2009)
X_V		Microbial density of the biofilm	Measured experimentally	0.4	$g\ cm^{-3}$	Liang et al. (2012)
$\frac{\mu_m}{Y}$	μ_m	Maximum specific growth rate of biomass	$\mu_m = \frac{\mu s}{s + K_s}$	$9.8 * 10^{-5}$	s^{-1}	Liang et al. (2012)
	Y	Yield coefficient of micro-organisms				

7. Conclusion

In this paper, the system of nonlinear differential equations on nitric oxide removal in a biotrickling filter has been solved analytically. The model investigated the influence of parameters over the removal of NO from the oxygen in the BTF reactor under thermophilic conditions. Approximate analytical expressions pertaining to the concentration of NO in the gas phase and the biofilm phase for all values of the parameters are obtained using the Adomian decomposition method. Our results are compared with the numerical simulation and it gives satisfactory agreement .This analytical result helps us for the better understanding of the model.

Nomenclature

Parameters

C_g	NO concentration in the gas phase, g cm^{-3}
C_l	NO concentration in the biofilm phase, g cm^{-3}
$C_{g,0}$	Inlet NO concentration, g cm^{-3}
U_g	Superficial gas velocity, cm s^{-1}
a_f	Specific surface area of biofilm, cm^{-1}
a_0	Specific surface area of medium, m^{-1}
D_e	Effective diffusion coefficient in the biofilm, cm^2 s^{-1}
k_g	Reaction rate constant, L^2 mol^{-2} s^{-1}
L_f	Biofilm thickness, cm
X_V	Microbial density of the biofilm, g cm^{-3}
K_s	Monod half saturation constant, g cm^{-3}
μ_m	Maximum specific growth rate of biomass, s^{-1}
μ	Growth rate of biomass, s^{-1}
Y	Yield coefficient of micro-organisms, g gNO^{-1}
z	Height value which is calculated from the base of the packing materials, cm
x	Coordinate axis which is calculated from the surface of the biofilm, cm

Dimensionless parameters

ε_f	Porosity ratio of biofilm covered packing materials
ε_0	Porosity of medium
H	Henry constant at 50 °C
$\bar{C}_g = \frac{C_g}{C_{g,0}}$	Dimensionless NO concentration in the gas phase
$\bar{C}_l = \frac{C_l}{C_g/H}$	Dimensionless NO concentration in the biofilm phase
$\bar{x} = \frac{x}{L_f}$	Dimensionless height calculated from the base of the packing material
$\bar{z} = \frac{z}{L_f}$	Dimensionless parameter
$\alpha = L_f\sqrt{\frac{\mu_m}{Y}\frac{X_V}{D_e K_s}}$	Dimensionless parameter
$\gamma = \frac{a_f D_e}{HU_g}$	Dimensionless parameter
$\eta = \frac{\varepsilon_f k_g C_{g,0} L_f}{U_g}$	Dimensionless parameter
$m = \frac{\alpha^4}{3(1+\beta)^3} - \frac{\alpha^2}{(1+\beta)}$	Dimensionless parameter
NO_i	Initial NO concentration in the gas phase
NO_f	Final NO concentration in the gas phase
NO_R	NO removal ratio (NO removal efficiency)
L	Linear operator
A_n	Adomian polynomial

Appendix A. Basic concepts of the Adomian decomposition method (ADM)

Consider the non-linear differential equation

$$y'' + N(y) = g(x) \tag{A.1}$$

with boundary conditions

$$y(0) = A,\ y'(b) = B \tag{A.2}$$

where $N(y)$ is a nonlinear function, $g(x)$ is the given function and A, B, b are given constants. We propose the new differential operator, as below

$$L = \frac{d^2}{dx^2} \tag{A.3}$$

So, Eq. (A.1) can be written as

$$L(y) = g(x) - N(y) \tag{A.4}$$

The inverse operator L^{-1} is therefore considered as a twofold integral operator (Duan and Rach, 2011;), as below

$$L^{-1}(.) = \int_0^x \int_b^x (.)dxdx \tag{A.5}$$

Applying the inverse operator L^{-1} on both sides of Eq. (A.4) yields

$$y(x) = L^{-1}(g(x)) - L^{-1}(N(y)) + y'(b)(x-0) + y(0), \tag{A.6}$$

Using the boundary conditions Eq. (A.2), Eq. (A.6) becomes

$$y(x) = L^{-1}(g(x)) - L^{-1}(N(y)) + Bx + A, \tag{A.7}$$

The Adomian decomposition method introduces the solution $y(x)$ and the nonlinear function $N(y)$ by infinite series

$$y(x) = \sum_{n=0}^{\infty} y_n(x) \tag{A.8}$$

and

$$N(y) = \sum_{n=0}^{\infty} A_n \tag{A.9}$$

where the components $y_n(x)$ of the solution $y(x)$ will be determined recurrently and the Adomian polynomials A_n of $N(y)$ are evaluated using the formula

$$A_n(x) = \frac{1}{n!}\frac{d^n}{d\lambda^n} N\left(\sum_{n=0}^{\infty} \lambda^n y_n\right)_{\lambda=0} \tag{A.10}$$

which gives

$$\begin{aligned} A_0 &= N(y_0) \\ A_1 &= N'(y_0)y_1, \\ A_2 &= N'(y_0)y_2 + \tfrac{1}{2}N''(y_0)y_1^2, \\ A_3 &= N'(y_0)y_3 + N''(y_0)y_1y_2 + \tfrac{1}{3!}N'''(y_0)y_1^3. \\ &\vdots \end{aligned} \tag{A.11}$$

By substituting Eqs. (A.8) and (A.9) in Eq. (A.7) gives

$$\sum_{n=0}^{\infty} y_n = L^{-1}(g(x)) - L^{-1}\left(\sum_{n=0}^{\infty} A_n\right) + Bx + A \tag{A.12}$$

Then equating the terms in the linear system of Eq. (A.11) gives the recurrent relation

$$y_0 = L^{-1}(g(x)) + Bx + A, \qquad y_{n+1} = -L^{-1}(A_n), \quad n \geqslant 0 \tag{A.13}$$

which gives

$$\begin{aligned} y_0 &= L^{-1}(g(x)) + Bx + A, \\ y_1 &= -L^{-1}(A_0), \\ y_2 &= -L^{-1}(A_1), \\ y_3 &= -L^{-1}(A_2), . \\ &\vdots \end{aligned} \tag{A.14}$$

From Eqs. (A.11) and (A.14), we can determine the components $y_n(x)$, and hence the series solution of $y_n(x)$ in Eq. (A.7) can be immediately obtained.

Appendix B. Analytical solution of dimensionless NO concentration in the biofilm phase

The solutions of Eq. (7) and (8) allow us to predict the concentration profiles of NO in the gas phase and the biofilm phase. In order to solve Eq. (7), we have to solve Eq. (8) using the Adomian decomposition method, Eq. (8) can be written in the operator form,

$$L(\bar{C}_l) = \alpha^2 N(\bar{C}_l) \tag{B.1}$$

where the differential operator $L = \frac{d^2}{d\bar{x}^2}$ and $N(C_l) = \frac{C_l}{1+\beta C_l}$

Applying the inverse operator

$$L^{-1}(.) = \int_0^{\bar{x}} \int_1^{\bar{x}} (.)d\bar{x}d\bar{x} \tag{B.2}$$

on both sides of Eq. (B.1) yields

$$\bar{C}_l(\bar{x}) = B\bar{x} + A + \alpha^2 L^{-1}\left[\frac{\bar{C}_l}{1+\beta\bar{C}_l}\right] \tag{B.3}$$

where $B = \bar{C}_l\prime(1)$ and $A = \bar{C}_l(0)$. We let,

$$\bar{C}_l(\bar{x}) = \sum_{n=0}^{\infty} \bar{C}_{l_n}(\bar{x}) \tag{B.4}$$

$$N[\bar{C}_l(x)] = \frac{\bar{C}_l}{1+\beta\bar{C}_l} = \sum_{n=0}^{\infty} A_n \tag{B.5}$$

In view of Eqs. (B.4) and (B.5), Eq. (B.3) gives

$$\sum_{n=0}^{\infty} \bar{C}_{ln}(\bar{x}) = B\bar{x} + A + \alpha^2 L^{-1}\sum_{n=0}^{\infty} A_n \tag{B.6}$$

We identify the zeroth component as

$$\bar{C}_{l_0}(\bar{x}) = B\bar{x} + A \tag{B.7}$$

and the remaining components as the recurrence relation

$$C_{ln+1}(x) = \alpha^2 L^{-1} A_n, n \geqslant 0 \tag{B.8}$$

where A_n are the Adomian polynomials of $\bar{C}_{l_1}, \bar{C}_{l_2} \cdots \bar{C}_l n$. We can find the first few A_n as follows:

$$A_0 = N(\bar{C}_{l_0}) = \frac{\bar{C}_{l_0}}{1+\beta\bar{C}_{l_0}} \tag{B.9}$$

$$A_1 = \frac{d}{d\lambda}[N(\bar{C}_{l_0} + \lambda\bar{C}_{l_1})]|_{\lambda=0} = \frac{\bar{C}_{l_1}}{(1+\beta)^2} \tag{B.10}$$

The remaining polynomials can be generated easily, and so,

$$\bar{C}_{l_0}(\bar{x}) = 1 \tag{B.11}$$

$$\bar{C}_{l_1}(\bar{x}) = \frac{\alpha^2\bar{x}(\bar{x}-2)}{2(1+\beta)} \tag{B.12}$$

$$\bar{C}_{l_2}(x) = \frac{\alpha^4 x[\bar{x}^2(x-4)+8)]}{24(1+\beta)^3} \tag{B.13}$$

Adding (B.11), (B.12), (B.13), we get Eq. (13) in the text.

References

Adomian, G., 1984. Convergent series solution of nonlinear equations. J. Computat. Appl. Math. 11, 225–230.

Baltzis, B.C., Mpanias, C.J., Bhattacharya, S., 2001. Modelling the removal of VOC mixtures in biotrickling filters. Biotechnol. Bioeng. 72 (4), 389–401.

Baquerizo, Guillermo et al, 2005. A detailed model of a biofilter for ammonia removal: Model parameters analysis and model validation. Chem. Eng. J. 113, 205–214.

Caceres, M., Silva, J., Morales, M., San, R.M., Aroca, G., 2012. Kinetics of the biooxidation of volatile reduced sulphur compounds in a biotrickling filter. Bioresour. Technol. 118, 243–248.

Chen, J., Wang, J., Ma, J., 2006. Effects of gas flow-rate and inlet concentration on nitric oxide removal in an autotrophic biofilter. J. Chem. Technol. Biotechnol. 81 (5), 812–816.

Cox, H.H.J., Sexton, T., Shareefdeen, Z.M., Deshusses, M.A., 2001. Thermophilic biotrickling filtration of ethanol vapors. Environ. Sci. Technol. 35, 2612–2619.

Cox, H.H., Deshusses, M.A., 1998. Biological waste air treatment in biotrickling filters. Curr. Opinion Biotechnol. 9, 256–262.

Deshusses Marc, A., et al., 2004. Odorous compounds emissions from biotrickling filters at wastewater treatment plants. Proceedings of the Water Environment Federation, WEF/A&WMA Odors and Air Emissions, pp. 265–276 (12).

Devinny, J S, Deshusses, M A, Webster, T S, 2002. Biofiltration for Air Pollution Control. CRC- Lewis Publishers, Boca Raton, FL.

Duan, J.S., Rach, R., 2011. A new modification of the Adomian decomposition method for solving boundary value problems for higher order nonlinear differential equations. Appl. Math. Comput. 218, 4090–4118.

Flanagan, W.P., Apel, W.A., Barnes, J.M., Lee, B.D., 2002. Development of gas phase bioreactors for the removal of nitrogen oxides from synthetic flue gas streams. Fuel 81 (15), 1953–1961.

Islam, G.M.R., Alam, M.J.B., 2006. NO_x removal from air by nitrosomonas europaea. Proc. Pak. Acad. Sci. 43 (4), 249–255.

James, G.C., Natalve, S., 1996. Microbiology (A Laboratory Manual). The Benjamin/Cummings Publishing Co., India, pp. 96–122.

Lee, B.D., Apel, W.A., Smith, W.A., 2001. Oxygen effects on thermophilic microbial populations in biofilters treating nitric oxide containing off-gas streams. Environ. Prog. 20 (3), 157–166.

Vafajoo, Leila, Naserranjbar, Ali, Khorasheh, Farhad, 2012. In: A Mathematical Model for Removal of VOC's from Polluted Air Utilizing a Biofilter, Chemical Engineering Transactions, MATLAB 6.1, vol. 29. The MathWorks Inc., Natick, MA, p. 2000.

Muthukaruppan, S., Senthamarai, R., Rajendran, L., 2012. Modelling of immobilized glucoamylase kinetics by flow calorimetry. Int. J. Electrochem. Sci. 7, 9122–9137.

Mohamed, M.A., 2010. Comparison differential transformation technique with Adomian decomposition method for dispersive long-wave equations in (2 + 1)-dimensions. Appl. Appl. Math. 5, 148–166.

Nagase, H., Yoshihara, K.-I., Eguchi, K., Yokota, Y., Matsui, R., Hirata, K., Miyamoto, K., 1997. Characteristics of biological NOx removal from flue gas in a Dunaliella tertiolecta culture system. J. Ferment. Bioeng. 83 (5), 461–465.

Omar Jaradat, K., 2008. Adomian decomposition method for solving Abelian differential equations. J. Appl. Sci. 8, 1962–1966.

Patel, A., Serrano, Sergio E., 2011. New approaches to the propagation of nonlinear transients in porous media. J. Hydrol. 397, 202–209.

Liao, Qiang. et al, 2008. Measurements and modelling of heat generation in a trickling biofilters for biodegradation of a low concentration volatile organic compound (VOC). Chem. Eng. J. 140, 221–234.

Siddiqui, A.M., Hameed, M., Siddiqui, B.M., Ghori, Q.K., 2010. Use of Adomian decomposition method in the study of parallel plate flow of a third grade fluid. Commun. Nonlinear Sci. Numer. Simul. 15, 2388–2399.

Skeel, R.D., Berzins, M., 1990. A method for the spatial discretization of parabolic equations in one space variable. SIAM J. Sci. Statist. Comput. 11, 1–32.

Solomon, S., Qin, D., Manning, M., Chen, Z., Marquis, M., Averyt, K.B., Tignor, M., Miller, H.L. (Eds.), 2007. Contribution of Working Group I to the Fourth Assessment Report of the Intergovernmental Panel on Climate Change. Climate Change 2007: the Physical Science Basis. Cambridge University Press, Cambridge, United Kingdom and New York, NY, USA.

Song, J., Kinney, K.A., 2002. A model to predict long-term performance of vapor phase bioreactors: a cellular automaton approach. Environ. Sci. Technol. 36 (11), 2498–2507.

Stewart, P.S., 2003. Diffusion in biofilms. J. Bacteriol. 185 (5), 1485–1491.

Namihira, Takao, Tsukamoto, Shunsuke, Wang, Douyan, Katsuki, Sunao, Hackam, Reuben, Akiyama, Hidenori, Uchida, Yoshitaka, Koike, Masami, 2000. Improvement of NOx Removal Efficiency Using Short-Width Pulsed Power. IEEE Trans. Plasm. Sci. 28 (2).

Van Langenhove, H., Wuyts, E., Schamp, N., 1986. Elimination of hydrogen sulphide from odorous air by a wood bark biofilter. Water Res. 20, 1471–1476.

Liang, Wei, Huang, Shaobin, Yang, Yunlong, Jiang, Ran, 2012. Experimental and modelling study on nitric oxide removal in a biotrickling filter using *Chelatococcus daeguensis* under thermophilic condition. Bioresour. Technol. 125, 82–87.

Zarook, S.M., Shaikh, A.A., 1997. Analysis and comparison of biofilter modes. Chem. Eng. J. 65, 55–61.